Influence of depolarization field on polarization states in epitaxial ferroelectric thin films with nonequally biaxial misfit strains

Jie Wang and Tong-Yi Zhang*

Department of Mechanical Engineering
Hong Kong University of Science and Technology
Clear Water Bay, Kowloon, Hong Kong, China

Abstract

Depolarization field and misfit strain are two important factors that may greatly influence the properties of ferroelectric thin films. The effect of depolarization field on polarization states of single-domain ferroelectric thin films with nonequally biaxial in-plane misfit strains are studied in the present work by numerically solving three coupled Euler-Lagrange equations, which are derived from the minimization of total free energy. The misfit strain-misfit strain and thickness-misfit strain phase diagrams are constructed for single-domain $PbTiO_3$ thin films grown on tetragonal substrates with and without depolarization field. The depolarization field shifts the phase boundaries in the phase diagrams, leading to the contraction and expansion of the regions of out-of-plane and in-plane phases, respectively. For ferroelectric thin films with nonequally biaxial misfit strains, the depolarization field induces the phase transitions from orthorhombic phases to in-plane tetragonal phases.

* Corresponding author, Tel: (852) 2358-7192, Fax: (852) 2358-1543, E-mail: mezhangt@ust.hk

I. Introduction

With the remarkable progress in the epitaxial growth of thin films, ferroelectric thin films have been found wide applications in new generations of dynamic random access memories, nonvolatile memories, tunable microwave devices, and other microelectronic and electro-optic devices.[1-5] An epitaxial ferroelectric thin film may have different material properties from its bulk counterpart due to the existence of a stronger depolarization field and the lattice mismatch between the film and its substrate. For example, the depolarization field may suppress the ferroelectric property in ultra thin films and change the order of the phase transition.[6,7] The misfit strains between a ferroelectric thin film and its substrate can alter the equilibrium polarization states, shift the phase transition temperature, and change the phase transition order.[8]

A depolarization field may be induced by unscreened charges on the surface and interface of a ferroelectric thin film and/or by inhomogeneous polarization distribution in the film.[9] Under the short-circuit boundary condition, there are no charges on the surface and interface so that a depolarization field is generated only by inhomogeneously distributed polarizations. The inhomogeneity of polarizations is attributed to the so-called intrinsic surface effect of thin films, which can be expressed in terms of the extrapolation length in the phenomenological Landau-Devonshire theory.[10-11] The extrapolation length describes the distance from the surface of a thin film, at which the polarization will become zero. To describe an inhomogeneous polarization field, the polarization gradient energy should be included into the total free energy of a thin film. An equilibrium state of polarization can be determined by solving Euler-Lagrange equations, which are derived from minimizing the total free energy. Since analytical solutions to the Euler-Lagrange equations are barely possible even in one-dimensional cases, numerical calculations

have been performed to obtain the results for most cases[12-14].

Most published studies of ferroelectric thin films based on the Landau-Devonshire theory are only involved one polarization component perpendicular to[9,12,15 -17] or parallel to[13] the surface of a thin film. The uniaxial polarization simplification is not able to describe three-dimensional polarization states in thin films. In the literature, there are some works studying three-dimensional polarization phase diagrams of ferroelectric thin films.[14,18,19] However, these works do not consider the effect of depolarization field on the phase diagrams. Recently, Glinchuk *et al* [20] comprehensively studied three-dimensional polarization phase diagrams of ferroelectric thin films with the consideration of depolarization fields. In their model, the misfit strain is assumed to be related only to the surface polarization. There is an alternative approach to the misfit strain, in which the misfit strain induces internal stresses inside the film such that the strain energy should be included in the bulk Landau-Devonshire free energy. [8,14] In the present work, we take the alternative approach to investigate the polarization phase diagram of ferroelectric films.

Figure 1 schematically shows the studied system that a single domain ferroelectric film epitaxially grown on a thick tetragonal substrate and the film is under the short-circuit condition. The film/substrate interface is coherent. The non-equally biaxial misfit strains are induced by the lattice mismatch such that $\varepsilon_{11} = (b - a_0)/b$, $\varepsilon_{22} = (c - a_0)/c$, and other components of misfit strains are zero, where b and c are the substrate lattice parameters and a_0 is the cubic cell constant of the film at the free standing paraelectric state. The rectangular Cartesian system is set up with the x_3 axis perpendicular to the film/substrate interface. When the thickness of the

substrate is sufficiently larger than the film thickness, the two non-equally biaxial misfit strains will produce a two-dimensional sustained clamping or straining condition for the film.

II. Helmholtz free energy and Euler-Lagrange equations

Helmholtz free energy density of a ferroelectric thin film with homogeneous polarizations grown on a tetragonal substrate is given in Ref. [8, 19], which is obtained through Legendre transformation of the standard Landau – Devonshire energy. In the present study, we assume that polarizations vary only along the film thickness direction such that the average free energy is calculated from

$$\tilde{F} = \frac{1}{d}\int_0^d \left\{ f_{LD}(P_i, \varepsilon_{ij}) + f_G(P_{i,j}) + f_{dep}(P_i) \right\} dx_3, \tag{1}$$

where d is the film thickness, P_i denotes the ith component of polarization, which is a function of x_3 only, f_{LD}, f_G, and f_{dep} are the Helmholtz free energy density, the polarization gradient energy, and the depolarization energy density, respectively. The Helmholtz free energy density takes the form of

$$\begin{aligned} f_{LD} &= \alpha_1^* P_1^2(x_3) + \alpha_2^* P_2^2(x_3) + \alpha_3^* P_3^2(x_3) + \alpha_{11}^* [P_1^4(x_3) + P_2^4(x_3)] + \alpha_{33}^* P_3^4(x_3) \\ &+ \alpha_{12}^* P_1^2(x_3) P_2^2(x_3) + \alpha_{13}^* [P_2^2(x_3) P_3^2(x_3) + P_1^2(x_3) P_3^2(x_3)] + \alpha_{111} [P_1^6(x_3) + P_2^6(x_3) + P_3^6(x_3)] \\ &+ \alpha_{112} \left\{ P_1^4(x_3)[P_2^2(x_3) + P_3^2(x_3)] + P_2^4(x_3)[P_1^2(x_3) + P_3^2(x_3)] + P_3^4(x_3)[P_1^2(x_3) + P_2^2(x_3)] \right\} \\ &+ \alpha_{123} P_1^2(x_3) P_2^2(x_3) P_3^2(x_3) + \frac{s_{11}(\varepsilon_{11}^2 + \varepsilon_{22}^2) - 2 s_{12} \varepsilon_{11} \varepsilon_{22}}{2(s_{11}^2 - s_{12}^2)}, \end{aligned} \tag{2}$$

in which the renormalized coefficients α_{ij}^* and α_i^* are given by

$$\alpha_1^* = \alpha_1 - \frac{Q_{12}(s_{11}\varepsilon_{22} - s_{12}\varepsilon_{11}) + Q_{11}(s_{11}\varepsilon_{11} - s_{12}\varepsilon_{22})}{s_{11}^2 - s_{12}^2},$$

$$\alpha_2^* = \alpha_1 - \frac{Q_{12}(s_{11}\varepsilon_{11} - s_{12}\varepsilon_{22}) + Q_{11}(s_{11}\varepsilon_{22} - s_{12}\varepsilon_{11})}{s_{11}^2 - s_{12}^2},$$

$$\alpha_3^* = \alpha_1 - \frac{Q_{12}(\varepsilon_{11} + \varepsilon_{22})}{s_{11} + s_{12}},$$

$$\alpha_{11}^* = \alpha_{11} + \frac{1}{2}\frac{1}{s_{11}^2 - s_{12}^2}[(Q_{11}^2 + Q_{12}^2)s_{11} - 2Q_{11}Q_{12}s_{12}],$$

$$\alpha_{33}^* = \alpha_{11} + \frac{Q_{12}^2}{s_{11}+s_{12}},$$

$$\alpha_{12}^* = \alpha_{12} - \frac{1}{s_{11}^2 - s_{12}^2}[(Q_{11}^2 + Q_{12}^2)s_{12} - 2Q_{11}Q_{12}s_{11}] + \frac{Q_{44}^2}{2s_{44}},$$

$$\alpha_{13}^* = \alpha_{12} + \frac{Q_{12}(Q_{11} + Q_{12})}{s_{11}+s_{12}}. \quad (3)$$

For a thin ferroelectric film, the polarization gradient energy density is reduced from the full gradient energy expression used in phase field models [21-24] and given by

$$f_G = \frac{1}{2}G_{11}\left(\frac{\partial P_3(x_3)}{\partial x_3}\right)^2 + \frac{1}{2}(G_{44} + G_{44}^{'})\left[\left(\frac{\partial P_2(x_3)}{\partial x_3}\right)^2 + \left(\frac{\partial P_1(x_3)}{\partial x_3}\right)^2\right]. \quad (4)$$

Only the polarization component perpendicular to the plane of thin film, i.e. P_3, can induce depolarization field. Thus, the depolarization field can be derived from Maxwell's equations[9,15] and given by $E_{d,3} = -\frac{1}{\varepsilon_0}\left[P_3(x_3) - \overline{P}_3\right]$ with the thickness-averaged polarization $\overline{P}_3 = \frac{1}{d}\int_0^d P_3(x_3)dx_3$. The depolarization energy density is then expressed by

$$f_{dep} = \frac{1}{2\varepsilon_0}\left[P_3(x_3) - \overline{P}_3\right]P_3(x_3). \quad (5)$$

In Eqs. (2)-(4), $\alpha_1 = (T - T_0)/2\varepsilon_0 C_0$ is the dielectric stiffness, α_{ij} and α_{ijk} are higher order dielectric stiffnesses, $\varepsilon_0 = 8.85\times10^{-12}$ Fm^{-1} is the dielectric constant of vacuum, T and T_0 denote temperature and the Curie-Weiss temperature, respectively, C_0 is the Curie constant; s_{ij} are the elastic compliance coefficients, Q_{ij} are electrostrictive constants, and G_{11}, G_{44} and $G_{44}^{'}$ are gradient coefficients. In the calculation, $G_{11} = 3.46\times10^{-10}\ m^4N/C^2$, $G_{44} = G_{44}^{'} = 1.73\times10^{-10}\ m^4N/C^2$ and other parameters for $PbTiO_3$ films are tabulated in Table I.[8,21] Note that the present thermodynamic model is able to predict the distribution of inhomogeneous polarizations in the thickness direction. If polarizations are homogeneous in the thickness direction, the gradient energy and the depolarization field will vanish and Eq. (1) will be reduced to the Helmholtz free energy in Ref. [19].

The equilibrium polarization distribution is determined by minimizing the total free energy of Eq. (1). Taking the functional variation of Eq. (1) with respect to polarizations $P_1(x_3)$, $P_2(x_3)$ and $P_3(x_3)$ yields the following three coupled nonlinear Euler-Lagrange equations

$$0 = 2\alpha_1^* P_1 + 4\alpha_{11}^* P_1^3 + 2\alpha_{12}^* P_1 P_2^2 + 2\alpha_{13}^* P_1 P_3^2 + 6\alpha_{111} P_1^5 + \alpha_{112}[4P_1^3(P_2^2 + P_3^2) + 2P_2^4 P_1 + 2P_3^4 P_1] + 2\alpha_{123} P_1 P_2^2 P_3^2 - (G_{44} + G_{44}^{'})P_{1,33}\ , \tag{6a}$$

$$0 = 2\alpha_2^* P_2 + 4\alpha_{11}^* P_2^3 + 2\alpha_{12}^* P_2 P_1^2 + 2\alpha_{13}^* P_2 P_3^2 + 6\alpha_{111} P_2^5 + \alpha_{112}[4P_2^3(P_1^2 + P_3^2) + 2P_1^4 P_2 + 2P_3^4 P_2] + 2\alpha_{123} P_2 P_1^2 P_3^2 - (G_{44} + G_{44}^{'})P_{2,33}\ , \tag{6b}$$

$$0 = 2\alpha_3^* P_3 + 4\alpha_{33}^* P_3^3 + 2\alpha_{13}^* P_3 (P_1^2 + P_2^2) + 6\alpha_{111} P_3^5 + \alpha_{112}[4P_3^3(P_1^2 + P_2^2) + 2P_1^4 P_3 + 2P_2^4 P_3] + 2\alpha_{123} P_3 P_1^2 P_2^2 - G_{11} P_{3,33} + \frac{P_3}{\varepsilon_0} - \frac{1}{d\varepsilon_0}\int_0^d P_3(x_3)dx_3\ , \tag{6c}$$

with the boundary conditions of

$$\left(\frac{\partial P_i}{\partial x_3} \pm \frac{P_i}{\delta} \right)\Bigg|_{x_3=0,\, d} = 0 \quad (i = 1,2,3), \tag{6d}$$

in which δ is the extrapolation length, and P_i denotes $P_i(x_3)$ and $P_{i,33}$ denotes the second derivative of the *i*th component of the polarization with respect to the coordinate x_3. The value of δ should be determined by first-principles calculations and/or by carefully designed experiments, which will be the future task of research. Currently, various values of δ are approximately used in the literature. The value of the extrapolation length, δ = 3 nm[25], is used for the three components of polarizations at the film surface and the interface between the film and the substrate in the present study. We employ finite difference with 100 discrete elements along the thickness to solve the above coupled nonlinear Euler-Lagrange equations numerically.

III. Misfit strain-misfit strain and thickness-misfit strain phase diagrams of epitaxial $PbTiO_3$ thin films

A. The effect of depolarization field on misfit strain-misfit strain phase diagrams

The equilibrium polarization distribution in a ferroelectric thin film with non-equally biaxial misfit strains is determined by numerically solving the Euler-Lagrange equations. Figures 2(a) and 2(b) show the thickness-averaged polarizations of $\overline{P_1}$ and $\overline{P_3}$, which are calculated from $\overline{P_i} = \frac{1}{d}\int_0^d P_i(x_3)dx_3$, at room temperature, respectively, in 8-nm-thick $PbTiO_3$ thin films as a function of misfit-strains, when the depolarization field is considered. Most values of the average polarization of $\overline{P_1}$ are nonzero if the misfit strain of ε_{11} is in tension, as shown in Fig. 2(a). Figure 2 (b) illustrates that the average polarization of $\overline{P_3}$ is nonzero when both misfit strains ε_{11} and ε_{22} are compressive, because the in-plane compressive misfit strains make the out-of-plane

polarization more preferable in free-energy reduction. Since the thickness-averaged polarizations $\overline{P}_2$ and $\overline{P}_1$ are symmetrical with respect to the plane of $\varepsilon_{11} = \varepsilon_{22}$ in the 3-dimensional plot of Fig. 2(a), the average polarization of $\overline{P}_2$ is not given here for simplicity. From the transition lines in Figs. 2(a) and 2(b), cross which the average polarizations change from zero to nonzero values, we construct misfit strain-misfit strain phase diagrams.

We introduce the following notations for different equilibrium phases, which may exist in the films: (i) the a_1 phase, where $\overline{P}_1 \neq 0$ and $\overline{P}_2 = \overline{P}_3 = 0$; (ii) the a_2 phase, where $\overline{P}_2 \neq 0$ and $\overline{P}_1 = \overline{P}_3 = 0$; (iii) the c phase, where $\overline{P}_3 \neq 0$ and $\overline{P}_1 = \overline{P}_2 = 0$; (iv) the a_1c phase, where $\overline{P}_3 \neq 0$ $\overline{P}_1 \neq 0$ and $\overline{P}_2 = 0$; (v) the a_2c phase, where $\overline{P}_3 \neq 0$, $\overline{P}_2 \neq 0$ and $\overline{P}_1 = 0$; (vi) the a_1a_2 phase, where $\overline{P}_1 \neq 0$, $\overline{P}_2 \neq 0$ and $\overline{P}_3 = 0$, and the the aa phase when $\overline{P}_1 = \overline{P}_2$ in this case; (vii) the r phase, where $\overline{P}_3 \neq 0$, $\overline{P}_1 \neq 0$ and $\overline{P}_2 \neq 0$. Figures 3 shows the misfit strain - misfit strain phase diagrams of 8-nm-thick $PbTiO_3$ thin films with and without depolarization field at room temperature, where the solid and dot-dash lines denote the phase diagrams with and without the depolarization field, respectively. One monoclinic r phase, three orthorhombic a_1a_2, a_1c, and a_2c phases, and three tetragonal c, a_1, and a_2 phases show up in different regions of misfit strains in both cases with and without the depolarization field. The phase diagram with the depolarization field looks similar to that without the depolarization field. But, the depolarization field makes the phase boundaries shift such that the region of out-of-plane phase is reduced and the region of in-plane phases is extended. This is because the depolarization field is only dependent on the out-of-plane polarization component. For the same reason, the phase boundaries between in-plane phases are independent of the depolarization field. That is why the phase

boundary between the a_1 and a_1a_2 phases and the phase boundary between the a_2 and a_1a_2 phases are not shifted when the depolarization field is considered, as shown on the right-upper part of Fig. 3.

Figure 4 gives misfit strain - misfit strain phase diagrams of 8-nm-thick $PbTiO_3$ thin films with and without depolarization field at temperature 300 ^oC, where again the solid and dot-dash lines denote the phase diagrams with and without the depolarization field, respectively. Comparing Fig. 4 with Fig. 3 indicates that the trend of the effect of depolarization field on the phase diagram is the same at 300 ^oC as that at room temperature. Of course, the phase diagrams themselves are different to some extent due to the change in temperature. The shifts of phase boundaries induced by depolarization field are similar in both temperatures, thereby leading to a conclusion that the depolarization field reduces the region of the c phase in the phase diagrams regardless of the temperatures. To illustrate clearly the difference in phase diagrams at 300 ^oC and room temperature, we replot the phase diagrams with depolarization fields in Fig. 5 with the solid and dot-dash lines to denote the phase diagrams at room temperature and 300 ^oC, respectively. It is shown that the regions of the tetragonal a_1 and a_2 phases become larger and the region of the tetragonal *c* phase becomes smaller when the temperature increases from 25 ^oC to 300 ^oC. The regions of the monoclinic r phase and the three orthorhombic a_1a_2, a_1c, and a_2c phases are smaller when the temperature is higher. This result suggests that the tetragonal phases are more stable than the monoclinic phase and the orthorhombic phases in the strained ferroelectric thin films at a higher temperature. This finding is consistent with the known fact that the transition temperatures of the monoclinic phase and the orthorhombic phases are lower than that of the tetragonal phase in most ferroelectric materials.[26] The in-plane tetragonal a_1 or a_2

phase appears in the region where one misfit strain is compressive and the other is tensile or compressive, whereas the in-plane orthorhombic a_1a_2 phase only exists when the misfit strains are tensile in both directions. The non-equally biaxial misfit strains with a tensile component are necessary for the formation of the in-plane tetragonal a_1 and a_2 phases, which are forbidden when the misfit strains are equally biaxial, thereby suggesting that the non-equally biaxial misfit strains must be imposed on the ferroelectric films by their substrates in order to obtain the stable and desired in-plane tetragonal phases.

B. The effect of depolarization field on thickness-misfit strain phase diagrams

Figure 6 shows thickness–misfit strain phase diagrams for epitaxial $PbTiO_3$ single-domain thin films with and without depolarization field under equally biaxial misfit strains of $\varepsilon_{11} = \varepsilon_{22}$ at room temperature. Under equally biaxial misfit strains, three ferroelectric phases, namely the monoclinic *r* phase, the orthorhombic *aa* phase and the tetragonal *c* phase, appear at different ranges of thicknesses and misfit strains. For 8-nm-thick $PbTiO_3$ thin films, the *r* phase exists only within the range of tensile misfit strains from 0.002 to 0.008 and from 0.0029 to 0.0101, respectively, with and without the depolarization field. At higher values of tensile misfit strains, the *aa* phase is the equilibrium phase in the films. The *c* phase is thermodynamically stable in the films without misfit strains or with compressive misfit strains, as illustrated in Fig. 6. The depolarization field shifts the phase boundaries between the *r* and *c* phases and between the *aa* and *r* phases downtowards to the compressive strain side, as shown in Fig. 6.

Figure 7 shows thickness-misfit strain phase diagrams of single-domain $PbTiO_3$ ferroelectric thin films with the non-equally biaxial misfit strains of $\varepsilon_{11} = -\varepsilon_{22}$ at room temperature with and

without depolarization field, in which the solid and dot-dash lines denote the phase diagrams with and without the depolarization field, respectively. In the non-equally biaxial case of $\varepsilon_{11} = -\varepsilon_{22}$, the phase diagram is anti-symmetric with respect to the misfit strain line of $\varepsilon_{22} = 0$. The orthorhombic a_1c and a_2c phases appear and the monoclinic r phase disappears in the case of $\varepsilon_{11} = -\varepsilon_{22}$, in comparison with the case under equally biaxial misfit strains. The depolarization field shrinks the c phase region, as shown in Fig. 7, which is similar to that in the case of $\varepsilon_{11} = \varepsilon_{22}$. The results indicate that whatever the anisotropies of the misfit strains are, the depolarization fields reduce the c phase region in the thickness-misfit phase diagrams.

C. The effect of depolarization field on polarization profiles

As mentioned above, polarizations change themselves along the film thickness direction and depolarization fields affect greatly on the polarization field. Figures 8(a) and 8(b) show profiles of polarization components of $P_2(x_3)$ and $P_3(x_3)$ along the thickness direction with and without depolarization field, respectively, in a 8-nm-thick single-domain $PbTiO_3$ ferroelectric thin film at room temperatures under the non-equally biaxial misfit strains of $\varepsilon_{11} = -\varepsilon_{22} = -0.01$. When the depolarization field is taken into account, the out-of-plane polarization component $P_3(x_3)$ vanishes and there is only one in-plane polarization component $P_2(x_3)$, which is shown by solid lines in Figs. 8 (a) and (b). However, both out-of-plane polarization component $P_3(x_3)$ and in-plane polarization component are nonzero when the depolarization field is not taken into account in the calculation. The thickness-averaged values of the polarization component $P_2(x_3)$ are 0.5064 C/m^2 and 0.1952 C/m^2 with and without the depolarization field, respectively, thereby indicating that the polarization enhances the thickness-averaged value about 2.5 times.

Without considering the depolarization field, the thickness-averaged value of the polarization component $P_3(x_3)$ would be 0.5822 C/m^2 in the film, as shown in Fig. 8(b). When only $P_2(x_3)$ exists, we call it the a_2 phase, while when $P_2(x_3)$ and $P_3(x_3)$ co-exist, they form the a_2c phase. Thus, Figures 8(a) and 8(b) imply that the depolarization field causes the phase transition from the in-plane orthorhombic a_2c phase to the tetragonal a_2 phase in the stained ferroelectric thin film. This result is also indicated by the thickness-misfit strain phase diagrams of Fig. 7.

Figure 9 shows the distribution of the polarization magnitude, $P_s = \sqrt{P_1^2 + P_2^2 + P_3^2}$, along the thickness direction of the a_2 and a_2c phases, which components are shown in detail in Figs. 8(a) and 8(b). The magnitude of polarization with the depolarization field is smaller than the magnitude without the depolarization field although both profiles look almost the same. The thickness-averaged value of the magnitude is 0.5064 C/m^2 with depolarization field, while the thickness-averaged value of the magnitude is 0.6142 C/m^2 without depolarization field. The result shows that the depolarization field changes not only the polarization states in ferroelectric thin films, but also the polarization magnitude.

Figure 10(a) shows the distributions of polarization component $P_3(x_3)$ along the thickness direction of a 8-nm-thick $PbTiO_3$ ferroelectric film with and without depolarization field, respectively, at room temperature under $\varepsilon_{11} = \varepsilon_{22} = 0$, while Figure 10(b) shows the $P_3(x_3)$ distributions for a 4-nm-thick $PbTiO_3$ ferroelectric film under the same conditions. Without any misfit strains, i.e., $\varepsilon_{11} = \varepsilon_{22} = 0$, there is only one nonzero polarization component, $P_3(x_3)$, which is also shown in the thickness – misfit strain phase diagram of Fig. 7. From Figures 10 (a) and 10

(b), it is found that the depolarization field makes the polarization distributions more homogeneous along the thickness direction in both films. The phenominon is more significant in the 4-nm-thick film than that in the 8-nm-thick film, as shown by Figs 10 (a) and 10 (b). In addition, the depolarization field reduces the thickness-averaged values of the polarizations in both films. For the 8-nm-thick film, the thickness-averaged value is $\overline{P}_3$=0.6246 C/m^2 when the depolarization field is not taken into account, whereas the value is $\overline{P}_3$=0.6017 C/m^2 when the deplarization field is considered. For the 4-nm-thick film, the corresponding two values are 0.6090 C/m^2 and 0.5902 C/m^2, which are respectively smaller than those of the 8-nm-thick film. The difference in the thickness-averaged value of polarizations between different film thicknesses is attributed to the thickness effect, as described above. Nevertheless, the depolarization field causes the decrease in the out-of-plane polarization and the result is consistent with other theoretical predictions reported in the literature.[27]

IV. Concluding remarks

The present work systematically studies the polarization states of single-domain thin films grown on tetragonal substrates with and without depolarization field. The thermodynamic function expressed by Eqs. (1)-(5) is the theoretical fundation of single-domain thin films grown on tetragonal substrates with depolarization field. Three coupled Euler-Lagrange equations are derived from the function variation of the thermodynamic function with the short-circuited boundary condition. Simutaneously solving the three coupled Euler-Lagrange equations is a minimization process of the thermodynamic function. Single-domain $PbTiO_3$ thin films are taken as examples to construct the misfit strain- misfit strain diagrams and the thickness-misfit strain phase diagrams. The results clearly illustrate the change in the phase boundaries caused by the

depolarization field. The depolarization field reduces the region of the out-of-plane phase and increases the region of the in-plane phases in both misfit strain- misfit strain phase diagrams and thickness-misfit strain phase diagrams. Moreover, the depolarization field may induce the phase transition from the orthorhombic phases to the in-plane tetragonal phases in the ferroelectric thin films with nonequally biaxial misfit strains. This is because in the in-plane tetragonal phases there is no depolarization field in the thickness direction of the ferroelectric thin films, meaning that the depolarization field has no effect on the polarization instability of the in-plane tetragonal phases.

It is should be noted that single domain films are investigated in the present study. Real ferroelectric thin films may form multidomain structures with 180° or/and 90° domain walls so that the depolarization field is reduced.[28] However, when the film thickness is sufficiently small, the single domain structure will be predominent[23], thereby indicating that the results obtained from the present study may be more applicable to extra-thin ferroelectric films.

Acknowledgements

This work was fully supported by an RGC grant from the Research Grants Council of the Hong Kong Special Administrative Region, China.

References

[1] M.J. Dalberth, R.E. Stauber, J.C. Price, C.T. Roger, and D. Galt, Appl. Phys. Lett. **72**, 507 (1998).

[2] Q.X. Jia, A.T. Findikoglu, D. Reagor, P. Lu, Appl. Phys. Lett. **73**, 897 (1998).

[3] H. N. Lee, D. Hesse, N. Zakharov, and U. Gosele, Science **296**, 2006 (2002).

[4] C.H. Ahn, K.M. Rabe, and J.M. Triscone. Science **303**, 488 (2004).

[5] C.L. Chen, H.H. Feng, Z. Zhang, A. Brazdeikis, Z.J. Huang, W.K. Chu, C.W. Chu, F.A. Miranda, F.W. Van Keuls, R.R. Romanofsky, and Y. Liou, Appl. Phys. Lett. **75**,412 (1999).

[6] J. Junquera, and P. Ghosez, Nature **422**, 506 (2003).

[7] I.P. Batra, P. Wurfel, and B.D. Silverman, Phys. Rev. Lett. **30**, 384 (1973).

[8] N.A. Pertsev, A.G. Zembilgotov, and A.K. Tagantsev, Phys. Rev. Lett. **80**, 1988 (1998).

[9] M.D. Glinchuk, E.A. Eliseev, and V.A. Stephanovich, J. Appl. Phys. **93**, 1150 (2003).

[10] W.L. Zhong, Y.G. Wang, P.L. Zhang, and B.D. Qu, Phys. Rev. B **50**, 698 (1994).

[11] S. Li, J.A. Eastman, Z. Li, C.M. Foster, R.E. Newnham, and L.E. Cross, Physics Letters A **212**, 341 (1996).

[12] V.C. Lo, J. Appl. Phys. **94**, 3353 (2003).

[13] K.H. Chew, C.L. Wang, F.G. Shin, H.L.W. Chan, and D.R. Tilley, Solid State Communications **123**, 457 (2002).

[14] J. Zhang, Z. Yin, and M.S. Zhang, Phys. Lett. A **310**, 479 (2003).

[15] R. Kretschmer, and K. Binder, Phys. Rev. B **20**, 1065 (1979).

[16] Y.G. Wang, W.L. Zhong, and P.L. Zhang, Phys. Rev. B **51**, 5311 (1995).

[17] A.G. Zembilgotov, N.A. Pertsev, H. Kohlstedt, and R. Waser, J. Appl. Phys. **91**, 2247 (2002).

[18] A.G. Zembilgotov, N.A. Pertsev, and A.L. Kholkin, Phys. Rev. B **66**, 214108 (2002).

[19] J. Wang, and T.Y. Zhang, Appl. Phys. Lett. **86**, 192905 (2005).

[20] M.D. Glinchuk, A.N. Morozovska, and E.A. Eliseev, J. Appl. Phys. **99**, 114102 (2006).

[21] Y.L. Li, S.Y. Hu, Z.K. Liu, and L.Q. Chen, Appl. Phys. Lett. **81**, 427 (2002).

[22] J. Wang, S.Q. Shi, L.Q. Chen, Y.L. Li, and T.Y. Zhang, Acta. Mater. **52**,749 (2004).

[23] J. Wang, and T.Y. Zhang, Phys. Rev. B **730**, 144107 (2006).

[24] Y.L. Li, S.Y. Hu, Z.K. Liu, and L.Q. Chen, Acta. Mater. **50**, 395 (2002).

[25] K. Ishikawa, and T. Uemori, Phys. Rev. B **60**, 11841 (1999).

[26] M.E. Lines, and A.M. Glass, Principles and applications of ferroelectrics and related materials. Oxford : Clarendon press (1977).

[27] T. Lu, and W. Cao, Phys. Rev. B **66**, 024102 (2002).

[28] W.Y. Shih, W.H. Shih, and I.A. Aksay, Phys. Rev. B **50**, 15575 (1994).

Table I. The parameters used in the calculations for $PbTiO_3$ thin film

(α_1, α_{ij}, α_{ijk}, Q_{ij}, s_{ij} and T are in units $C^{-2}m^2N$, $C^{-4}m^6N$, $C^{-6}m^{10}N$, $C^{-2}m^4$, m^2N^{-1} and ^oC, respectively) [8]

α_1 $\times 10^5$	α_{11} $\times 10^6$	α_{12} $\times 10^8$	α_{111} $\times 10^8$	α_{112} $\times 10^8$	α_{123} $\times 10^9$	Q_{11}	Q_{12}	Q_{44}	s_{11} $\times 10^{-12}$	s_{12} $\times 10^{-12}$	s_{44} $\times 10^{-12}$
3.8(T-479)	-73	7.5	2.6	6.1	-3.7	0.089	-0.026	0.0675	8.0	-2.5	9.0

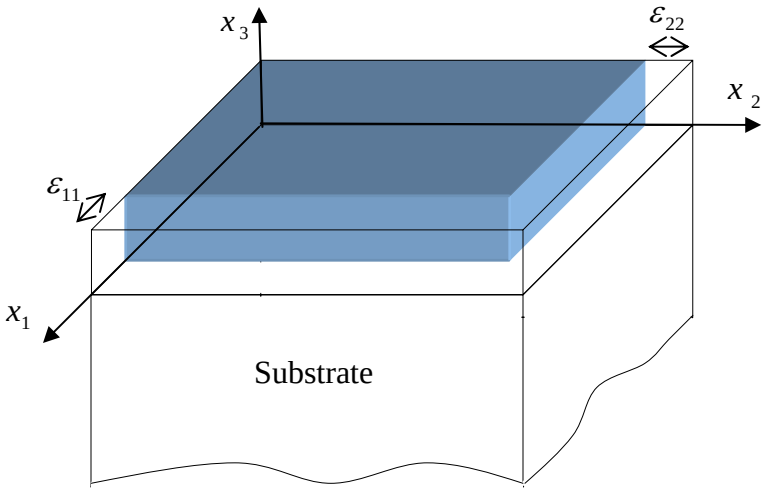

Fig.1. Schematic illustration of non-equally biaxial misfit strains of ε_{11} and ε_{22} in a single-domain ferroelectric thin film coherently deposited on an infinitely thick substrate, in which the top surface of the film and the interface between the film and the substrate are short-circuited.

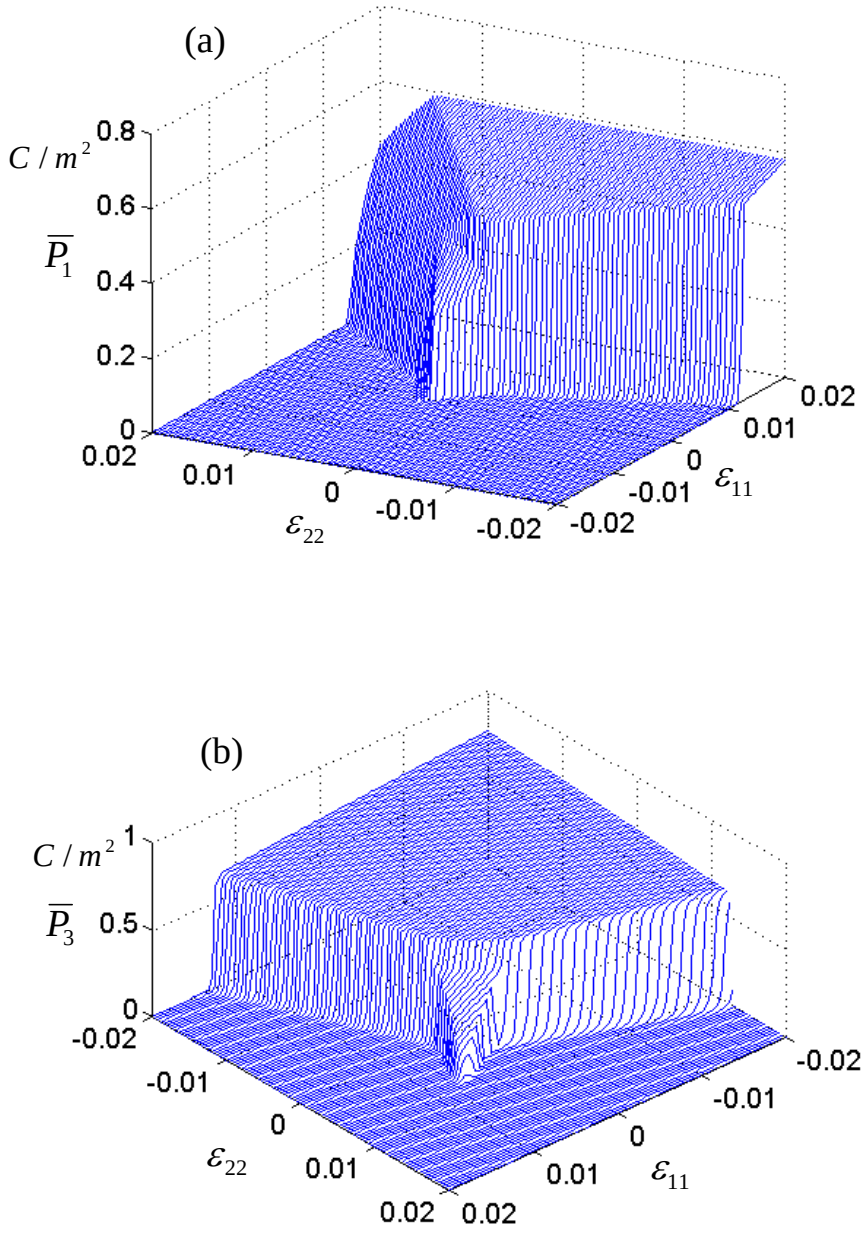

Fig.2. The thickness-averaged values of polarization components in a 8-nm-thick $PbTiO_3$ thin film with depolarization field at room temperature as a function of the misfit strains, the polarization components (a) in the x_1 direction and (b) in the x_3 direction.

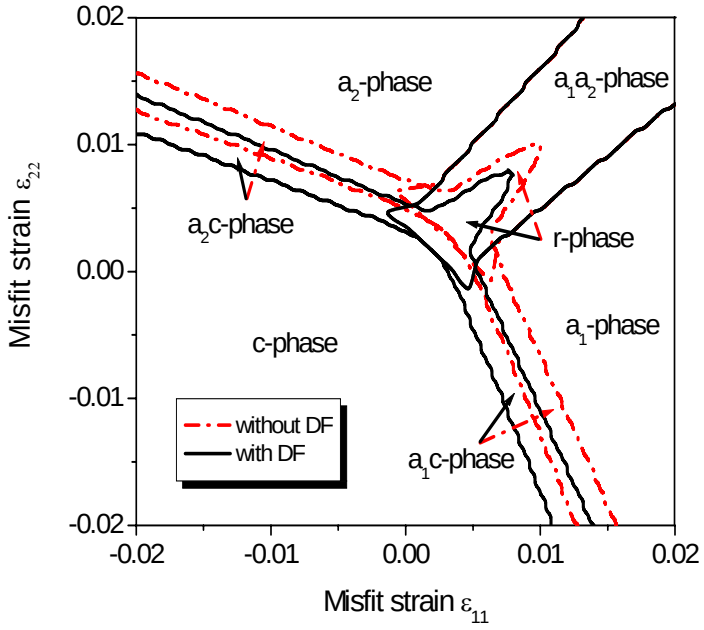

Fig.3. Misfit strain - misfit strain phase diagrams of 8-nm-thick $PbTiO_3$ thin films with and without depolarization field (DF) at room temperature.

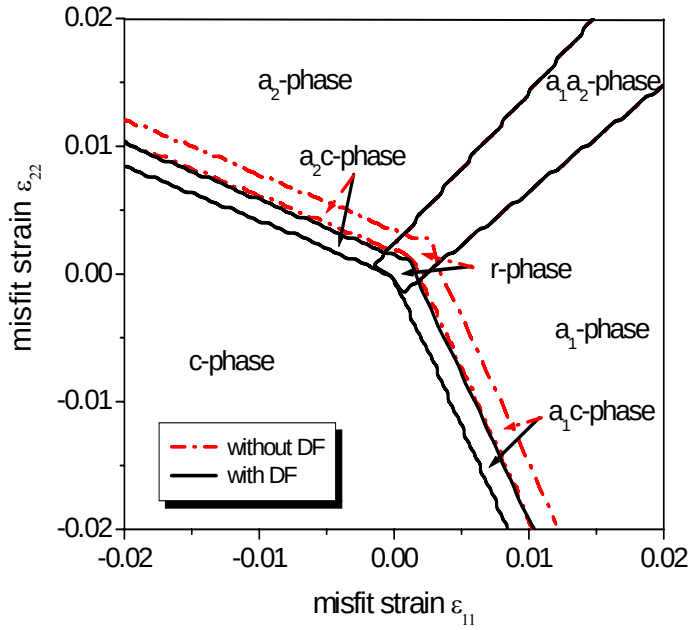

Fig.4. Misfit strain - misfit strain phase diagrams of 8-nm-thick $PbTiO_3$ thin films with and without depolarization field at the temperature of 300^{o}C.

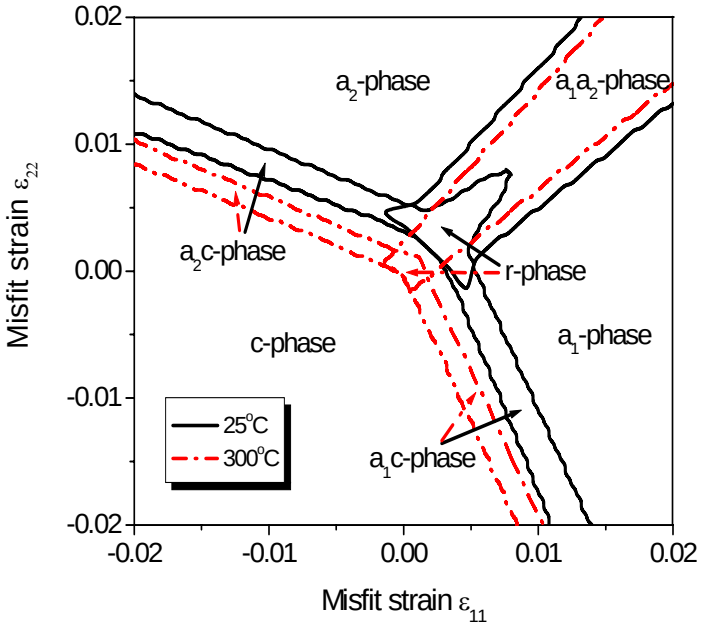

Fig.5. Misfit strain - misfit strain phase diagrams of 8-nm-thick $PbTiO_3$ thin films with depolarization field at 25 ° C and 300 ° C.

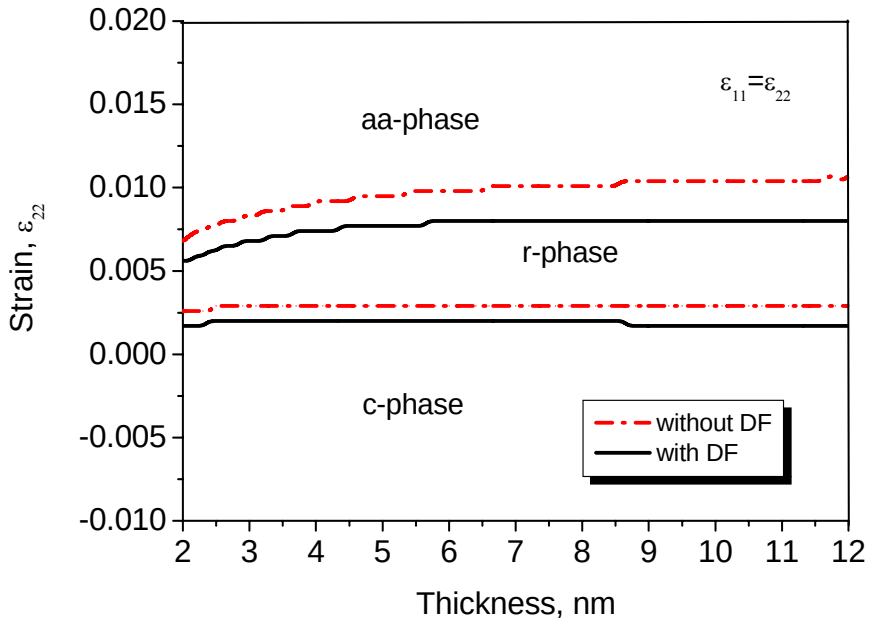

Fig.6. Thickness - misfit strain phase diagrams of $PbTiO_3$ thin films with and without depolarization field under misfit strains of $\varepsilon_{11} = \varepsilon_{22}$ at room temperature.

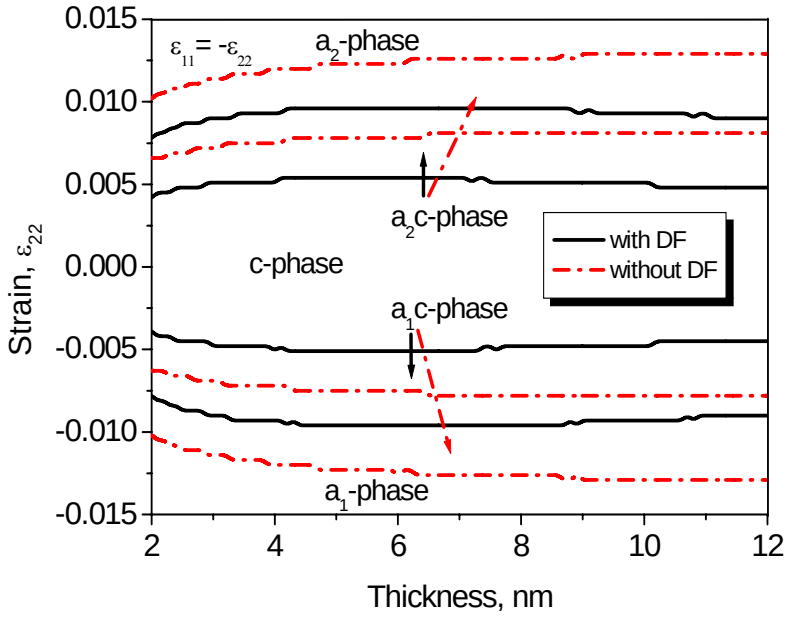

Fig.7. Thickness - misfit strain phase diagrams of $PbTiO_3$ thin films with and without depolarization field under misfit strains of $\varepsilon_{11} = -\varepsilon_{22}$ at room temperature.

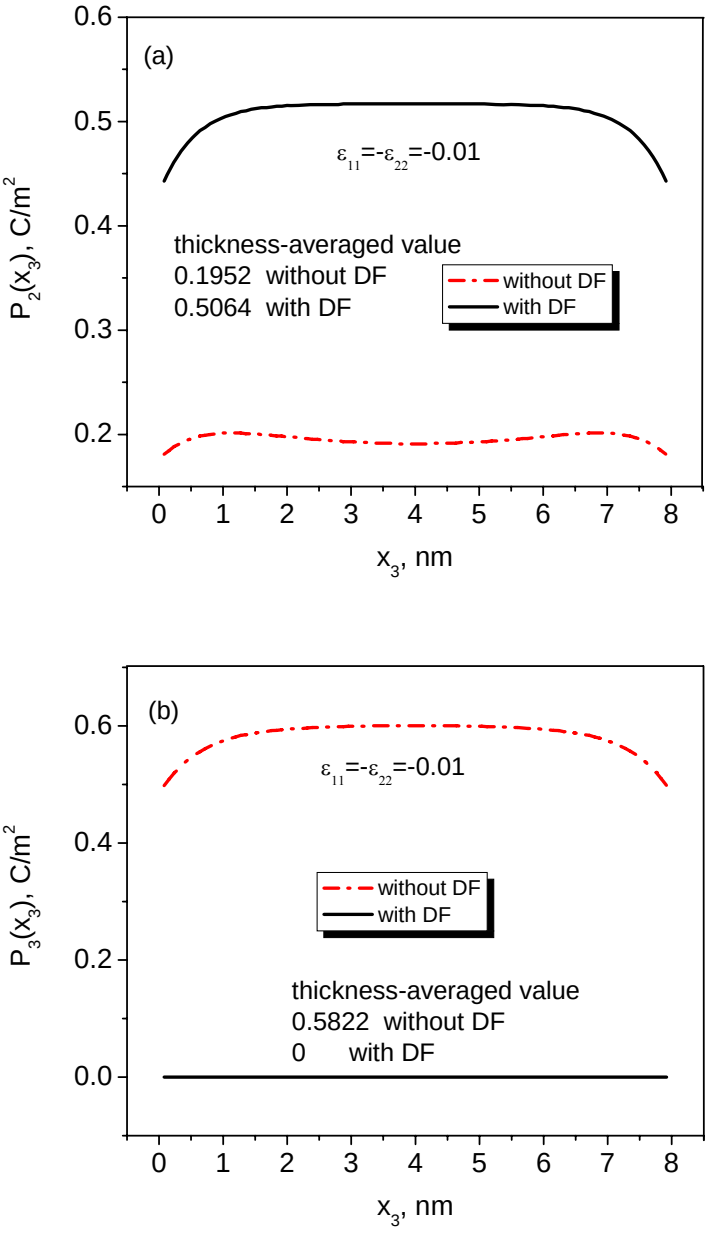

Fig.8. Profiles of polarization components along the thickness direction of 8-nm-thick $PbTiO_3$ thin films with and without depolarization field at room temperatures, (a) the polarization components in the x_2 direction and (b) in the x_3 direction.

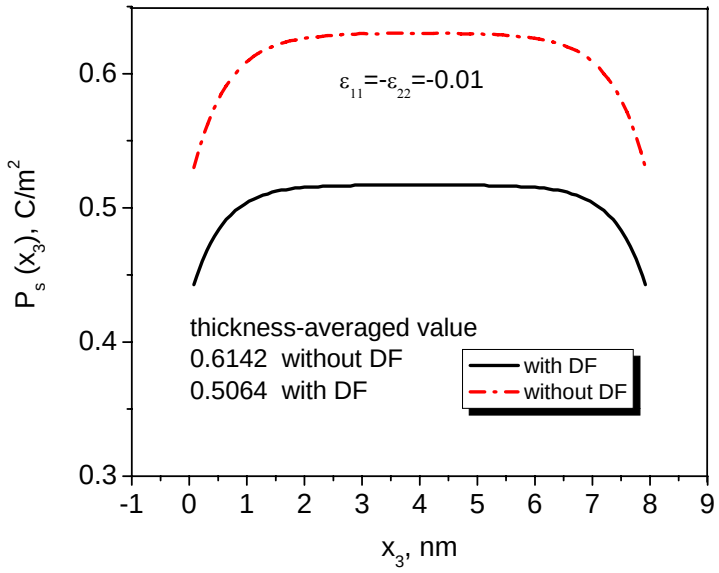

Fig.9. Profiles of polarization magnitudes along the thickness direction of 8-nm-thick $PbTiO_3$ thin films with and without depolarization field at room temperatures.

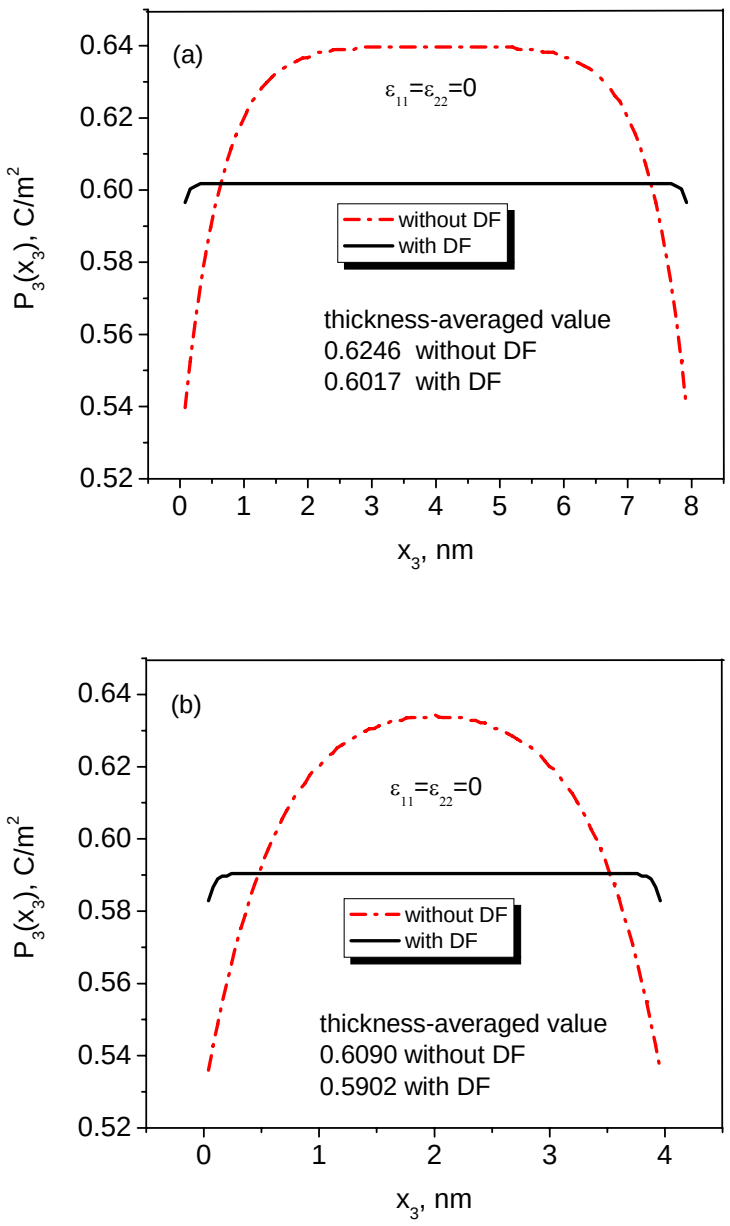

Fig.10. Profiles of polarization components along the thickness direction of $PbTiO_3$ thin films, with and without depolarization field at room temperatures, of film thicknesses of (a) 8 nm and (b) 4 nm.